Empirical Orthogonal Analysis of Pacific Sea Surface Temperatures

BRYAN C. WEARE, ALFREDO R. NAVATO AND REGINALD E. NEWELL

Department of Meteorology, Massachusetts Institute of Technology, Cambridge 02139

(Manuscript received 1 December 1975, in revised form 16 April 1976)

ABSTRACT

An empirical orthogonal function analysis has been performed on monthly mean sea surface temperatures for the greater part of the Pacific Ocean between 55°N and 20°S. The analysis identifies the most important modes of seasonal and non-seasonal variability during the period 1949–73. A mode is defined spatially in terms of an empirical orthogonal function which describes the degree of coherence of variation. The function's corresponding coefficients portray the evolution of the mode in time. The seasonal variation is dominated by a mode having a 12-month periodicity and greatest coherence in the higher latitudes. A second important seasonal mode has a period of approximately 6 months and is dominated by deviations in the North Pacific. The most important non-seasonal variation is identified with the long-recognized El Niño. The spatial pattern of this mode demonstrates the large-scale nature of the El Niño phenomenon. Other important non-seasonal modes are discussed.

1. Introduction

This study employs an empirical orthogonal function analysis to define a small number of variables which account for much of the spatial and temporal variability of sea surface temperatures of a large portion of the Pacific Ocean.

Empirical orthogonal function analysis enables fields of highly correlated data to be represented adequately by a small number of orthogonal functions and corresponding orthogonal time coefficients. Unlike most other orthogonal representations, such as the more familiar Fourier analysis, these functions do not require a predetermined form but, rather, depend upon the interrelationships within the data being analyzed. This property is especially important when investigating sea surface temperatures which do not have a known analytical form and which are subject to complex boundary conditions. Simply stated, the first of these functions is that linear combination of the original variables which, when used as a linear predictor of those variables, explains the greatest fraction of the total variance. Subsequent functions are required to account for the largest parts of the remaining variances (Lorenz, 1956). The first few functions, which together may explain a majority of the variance, and their time coefficients are often referred to as the principle model of variation. As in the case of the lower order Fourier components, these modes may have physical interpretations. This is largely because the orthogonality requirements are not very severe in that the coefficients may be, and indeed are, highly correlated at lags or leads of one or more months.

There are a number of examples of the application of empirical orthogonal function analysis to meteorological fields (e.g., Craddock and Flood, 1969; Rinne, 1971; Kidson, 1975a). Quite recently, the method has also been applied to sea surface temperatures (Trenberth, 1974; Weare *et al.*, 1975; Barnett and Davis, 1975).

Kutzbach (1967) provides a lucid outline of the mathematical procedure necessary to define the functions and their coefficients. A covariance (or correlation) matrix must be formed from the deviations of the data from a chosen mean. To maximize the variance explained by the new functions one must solve the system of linear equations associated with this matrix for a set of eigenvalues. These eigenvalues are the terms of the diagonalized covariance matrix. An eigenvalue divided by the sum of all the eigenvalues represents the fraction of the total variance in the original data field explained by its corresponding eigenfunction. A function is found by substituting a given eigenvalue into the system of equations and solving with the aid of an additional normalization condition. Associated with the functions are coefficients which, when combined with the functions, would provide for an exact reproduction of the original field if all functions and coefficients were used. These coefficients, which are orthogonal in time, are the result of the scalar product of the functions and the components of the original deviation field.

2. Data processing

The data used in this study are monthly mean sea surface temperatures covering the Pacific between 55°N and 20°S derived from summarizations of marine weather observations. For the period 1949–62 we calculated 5° grid averages from the analyses derived by Sette and his co-workers which were made available on

Unauthenticated | Downloaded 01/23/22 12:38 AM UTC

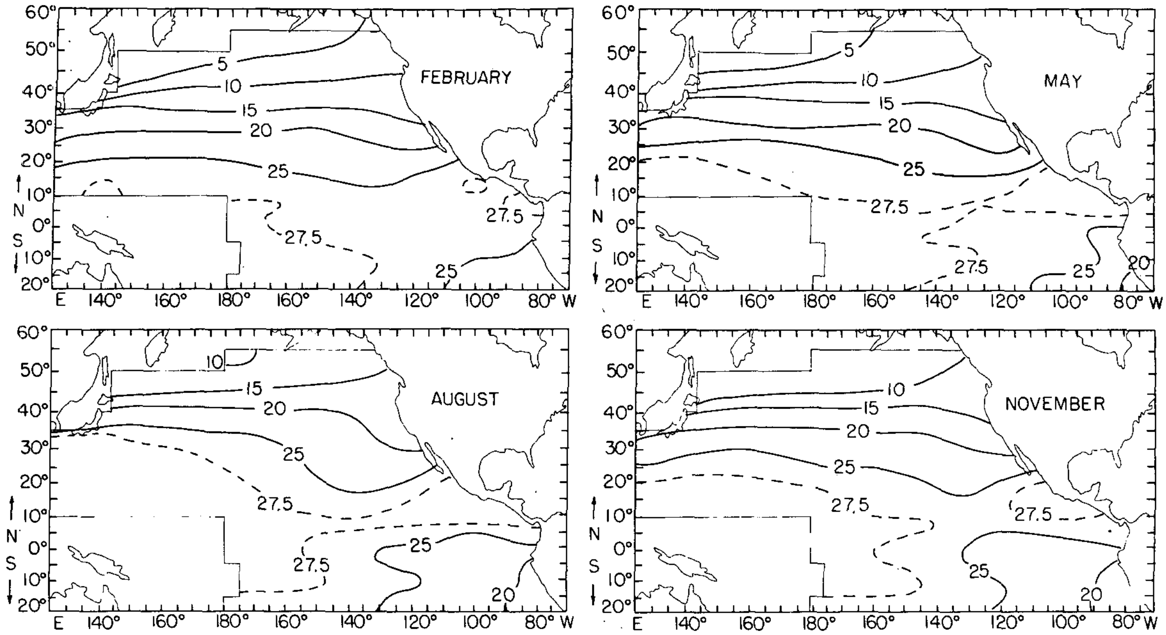

FIG. 1. Monthly mean sea surface temperatures (°C) derived from the entire record investigated (1949–73) for the months shown. Analyses of 5° latitude by 10° longitude grid points.

magnetic tape from the National Center for Atmospheric Research. These analyses are carefully corrected for individual ship biases, gross errors and analysis errors (Sette *et al.*, 1968). The data for the eastern, northern and tropical Pacific for 1963–73 were obtained from a tape of 5° grid averages of marine observations provided by L. E. Eber of the Southwest Fisheries Center. These data had undergone less processing to filter out errors. Both data bases have relatively sparse coverage south of the equator (generally averaging less than ten observations per month per 5° square). The western Pacific data for the latter period were obtained primarily from an interpolation of 5° grid point averages from the Ten Day Marine Reports summary maps published by the Japanese Meteorological Service. These do not cover the area below about 10°N and no comprehensive source was found for this region for the period after 1962.

All the data were reformatted to the 5° grid of the Fisheries data. In order to decrease the computation time, the number of points was reduced by averaging adjacent 5° squares giving a 10° longitude by 5° latitude array and by eliminating the area south of 10°N and west of 180°. The annual and monthly means for each grid were calculated for the entire 25 years of records. The data for each month of the 1963–73 period were printed in a map-like form and subjectively analyzed. Grids with no data in a month, but having at least two adjacent grids with data, were filled by adding to their long-term means the average of the deviations from the respective means of the reporting neighbors. Grids without two reporting neighbors and those with gross errors were set to their long-term means for the given month. No corrections were made to the 1949–62 analyses. The long-term means were recalculated. The differences between the "uncorrected" means and the "corrected" means are as large as 0.2°C in the sparse data areas of the eastern tropical Pacific.

We calculated deviations and hence empirical orthogonal functions which both included and excluded the seasonal cycle. For the seasonal calculations, which were performed first, the missing data interpolation scheme was not used. In both cases, deviations from the long-term mean were calculated. For the analysis which was to include the seasonal cycle, that mean was the mean annual average for all months. For that which was to exclude the seasonal cycle the mean was the long-term mean corresponding to the month in question. In both cases this procedure generates a 160×300 array of deviations from which a scalar product with itself forms a 160×160 covariance matrix. The matrices were diagonalized and the resulting eigenvalues ordered from largest to smallest. The eigenfunctions corresponding to the largest eigenvalues were calculated together with their time coefficients for each month.

3. Results

The long-term monthly means of sea surface temperature are illustrated in Fig. 1 for the sample months February, May, August and November. These analyses are drawn from the plotted 5° latitude by 10° longitude grid data. All the monthly means are quite similar, although not identical, to those published previously covering other periods (U. S. Navy, 1969). However,

Unauthenticated | Downloaded 01/23/22 12:38 AM UTC

TABLE 1. Percent and cumulative percent of total variance explained by the first 10 EOF's.

		1	2	3	4	5	6	7	8	9	10
	Seasonal EOF	1	2	3	4	5	6	7	8	9	10
A	Percent	81.7	4.6	2.2	1.6	.9	.8	.6	.5	.4	.4
	Cumulative percent	81.7	86.3	88.5	90.1	91.0	91.8	92.4	92.9	93.3	93.7
	Non-seasonal EOF	1	2	3	4	5	6	7	8	9	10
B	Percent	23.1	7.5	5.8	4.8	4.1	3.6	2.7	2.5	2.2	1.9
	Cumulative percent	23.1	30.6	36.4	41.2	45.3	48.9	51.6	54.1	56.3	58.2

a cooling trend was identified in the period studied by comparing the 1949–62 monthly means with those of 1963–73 (Weare *et al.*, 1975). The western Pacific is approximately 0.5°C warmer in the earlier period for all months except May when the differences are minimal. Changes in the eastern and tropical Pacific are less distinctive.

Fig. 2a indicates the variance pattern for the Pacific computed from the 300 months of deviations from the long-term annual mean. Since these deviations are primarily due to seasonal fluctuations the variance is greatest in the extratropical regions, especially near the fringes of the Kuroshio. Local maxima also occur in the upwelling regions off Baja California and Peru. The non-seasonal variance pattern calculated from deviations computed from the long-term monthly means is shown in Fig. 2b. The numerical values are much smaller than those of the seasonal case with a maximum near the coast of South America.

The percentages and cumulative percentages of total variance explained by the first ten empirical orthogonal functions which include the seasonal cycle are given in Table 1A; those for the functions excluding the seasonal cycle are given in Table 1B. The values are quite similar to those for the components of surface temperature and sea level pressure over the Northern Hemisphere computed by Kidson (1975a). The table suggests that four functions are probably adequate to describe seasonal variations for the entire Pacific Ocean analyzed. More functions are necessary to adequately represent non-seasonal variations. The questions as to how many functions should be considered in describing a system and how many of these represent noise are largely unanswered. Craddock (1973) has discussed a number of empirical criteria to answer the questions, none of which is wholly satisfactory. In addition, even the most important functions may poorly describe small areas of the field since the ranking of functions is based on summing the explained variance over all grids and this variance may differ considerably from point to point.

Figs. 3–10 display analyses of the spatial patterns and plots of the corresponding time coefficients for each of the most important seasonal and non-seasonal empirical orthogonal functions (EOF), designated S1, S2, ... and NS1, NS2, ..., respectively. In viewing these figures it should be remembered that, for a given

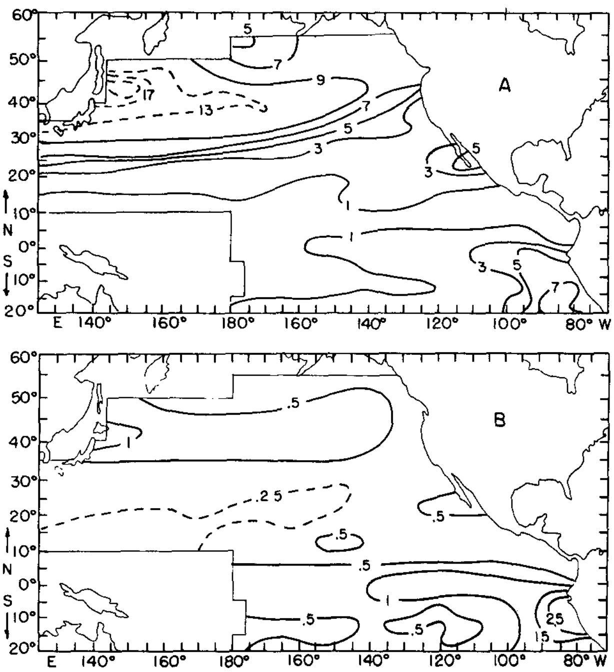

FIG. 2. Variances of deviations from long-term means for 1949–73: (a) deviations computed from mean annual average, (b) deviations computed from monthly means.

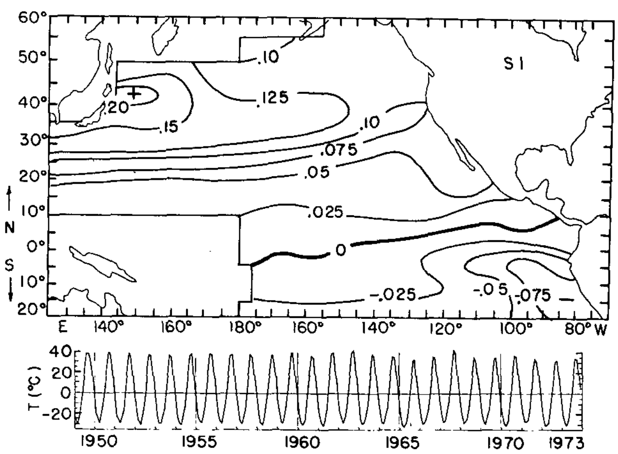

FIG. 3. Empirical orthogonal function S1, explaining 81.7% of total variance shown in Fig. 2a, together with its corresponding time coefficients. Function is based on departures from long-term annual averages. Tics in the time series identify January of the respective year starting with January 1949 and ending with December 1973.

Unauthenticated | Downloaded 01/23/22 12:38 AM UTC

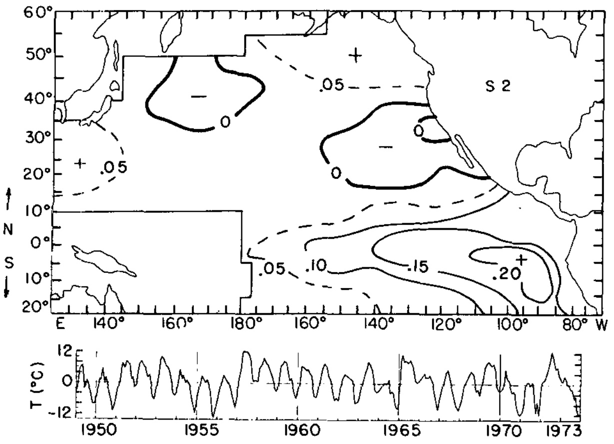

FIG. 4. S2 explaining 4.6% of the total variance as in Fig. 3.

function, any two regions vary in phase with a proportionality factor equal to the ratio of the values of the function in the regions. However, we will usually refer to regions as being anticorrelated if the factor is negative. In interpreting these figures it should be remembered that the contribution of a given mode to the temperature deviation from the chosen mean for a specified area and time is simply the product of the value of the function for that area and the value of that function's time coefficient for the month in question.

S1 (Fig. 3), explaining 81.7% of the variance, identifies the principal mode of seasonal changes. It is largest for grids in the vicinity of the most northern extent of the Kuroshio, indicating that this is the region of the largest seasonal variation. It is smallest in the tropical regions with the exception of a local maximum off the coast of South America having the opposite sign to the northern maximum, implying that these regions are quite strongly anticorrelated.

The second function S2 (Fig. 4), explaining 4.6% of the total variance, portrays coherent variation west of the Peru Current and along the Equatorial Current. The remainder of the Pacific considered undergoes relatively little variation in this mode although there is some coherence south of Japan and west of British Columbia. The time series corresponding to this function quite clearly shows the distinctive El Niño periods of 1957–58, 1965, 1969 and 1972 superimposed on a seasonal modulation. It also illustrates the colder than normal periods of 1949–50, 1954–56 and 1971. The strong 12-month periodicity of this time series and that of S1 illustrates how coefficients of the two orthogonal functions may be highly correlated in time at greater than zero lag.

The pattern of S3 (Fig. 5) is dominated by the strong zonal regions of opposite sign in the North Pacific. The resultant time series has a period of approximately 6 months and nearly constant amplitude. The line dividing these two regions is closely coincident with the average position of the North Pacific Current. In addition, the shapes of the regions quite clearly suggest the Aleutian and North Pacific Gyres. Function S4 appears to be dominated by east-west gradients of variation. The time series suggests a shift from a cooler to warmer regime in late 1956 in the eastern Pacific.

NS1 (Fig. 7), explaining 23.1% of the total non-seasonal variance, clearly corresponds to the seasonal EOF, S2, in that it displays the mode of variation characteristic of El Niño. However, in this case a much more coherent pattern in the extratropical regions is displayed, thus emphasizing the very large-scale character of El Niño. An interesting aspect of the large-scale nature of El Niño is the fact that the temperature near western North America varies in phase with that of the south equatorial Pacific, whereas a large region in the central North Pacific is anticorrelated. The time series of NS1 more clearly illustrates the known El Niño periods than that of S2, although the two series are quite similar if one removes the monthly means of the coefficients from the S2 series.

The spatial pattern of the second non-seasonal EOF (Fig. 8), explaining 7.5% of the total variance, emphasizes the North Pacific "center of action" of sea surface temperature whose variations Namias (1974) and Rogers (1974) have suggested are quite well correlated with weather anomalies over North America. In this mode, in contrast to NS1, deviations in the region just west of North America are anticorrelated with those near Peru. The magnitude and sign of the function in the latter region are comparable to those of the "center of action" suggesting that the scale of the sea surface anomalies influencing North American weather may be larger than hereto envisaged. The time series of NS2 shows distinctive changes in temperature in 1957–58, 1971 and 1972–73, each of which Namias (1972, 1973, 1974) has associated with changes in persistent weather patterns over North America. Equally large changes occur in other years such as 1954–55 and 1965–66.

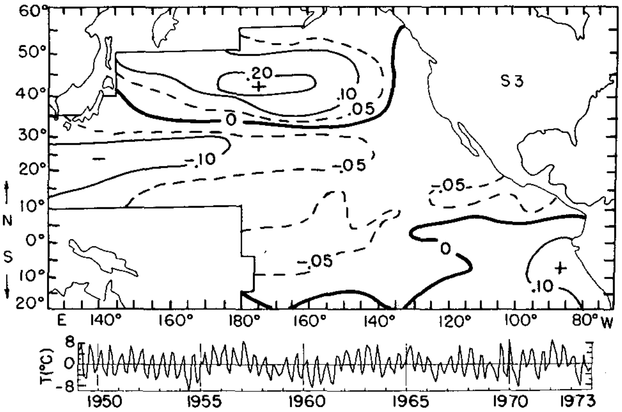

FIG. 5. S3 explaining 2.2% of the total variance as in Fig. 3.

Unauthenticated | Downloaded 01/23/22 12:38 AM UTC

The third non-seasonal EOF (Fig. 9) is much less coherent than the first two. The time series, however, clearly indicates a dramatic cooling late in 1962 in the western Pacific which is consistent with that observed by Iida *et al.* (1975). Indeed, the time series suggests persistent cool eras for this mode from 1963 through 1966 and from late in 1969 through 1973 for a large part of the western North Pacific. During the same periods the equatorial region was warmer than average. Although the difference between the pre-1963 and post-1963 regimes may be related to a change in data sources in January 1963 used in this study, Iida's results suggest that the source change probably does not bias the results substantially.

NS4 (Fig. 10) is dominated between about 45°N and the equator by a strong east-west pattern in which the east varies in the opposite sense of the west. As in the time series of the other non-seasonal EOF's, there appears to be considerable persistence in the temporal variations of this function. Before 1957 there is a period with temperatures which are relatively high in the west and low in the east. The period from around 1962 to late in 1968 seems to have the opposite characteristics. Although a substantial proportion of the variance is explained by patterns NS5-10, as seen from Table 1, for brevity we limit our discussion here to the first four functions.

4. Discussion

We have suggested that the most important empirical orthogonal functions arising from our analysis have physical interpretations in the sense that they have spatially coherent patterns and can be associated, at least qualitatively, with known phenomena or hypothetical causal mechanisms. Such interpretability can only arise, however, when the length of record and areal extent of data coverage are sufficiently large. For example, one would not expect to be able to identify the El Niño mode if only the North Pacific were considered, or if the record length corresponded to only a half-period or less of this quasi-cyclic phenomenon. Furthermore, one may only speak in terms of successions of interacting events of these modes, which are constrained in space and time to be orthogonal at zero lag, for phenomena which have characteristic times greater than one month.

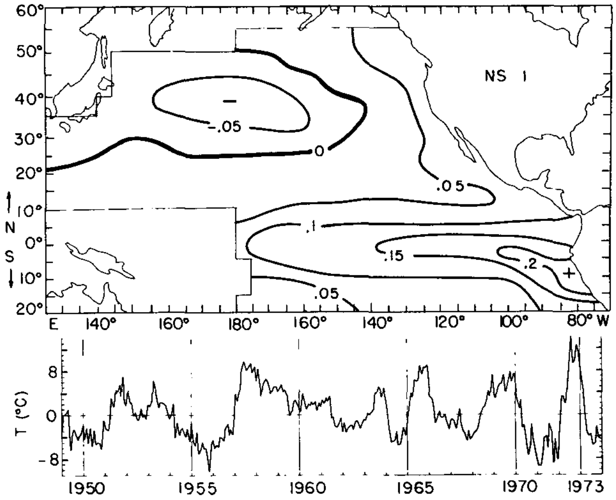

FIG. 7. As in Fig. 3 except for empirical orthogonal function NS1, explaining 23.1% of the total variance in the Fig. 2b.

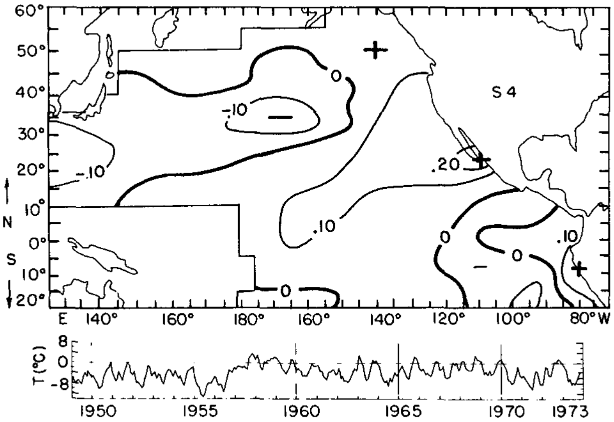

FIG. 6. S4 explaining 1.6% of the total variance as in Fig. 3.

The physical factors involved in the month-to-month sea surface temperature changes at a given place have been discussed by Clark (1967, 1972) and other authors. Basically the water temperature changes by two categories of processes: those acting through the surface such as net radiative heating or cooling, evaporative or latent heat transfer and sensible heat transfer; and those acting within the water mass, such as horizontal advection by various scales of motion, and vertical advection.

The most obvious known phenomenon in our results is the seasonal variation which dominates S1 (Fig. 3). Even in this case the detailed explanation of the pattern is by no means simple. In summer in the North Pacific, when the ocean is being heated by the sun, the Kuroshio carries warm water further poleward and the Oyashio and the North Pacific subpolar gyre are relatively weak as they are under the influence of weak winds (Hellerman, 1967). Horizontal advection and radiation are thus likely to be the main contributors to the summer rise of temperature in the positive region of S1. In the winter the situation is largely reversed. The Kuroshio moves to the south and the Oyashio and Aleutian Current are strengthened due to stronger winds in the high latitudes. In addition, water off Japan is cooled by the loss of large amounts of sensible and latent heat to the cold dry air streaming off the Asian continent. The pattern of S1 indicates that in association with the warm water in the North Pacific in August there is relatively cold water off South America and south of

Unauthenticated | Downloaded 01/23/22 12:38 AM UTC

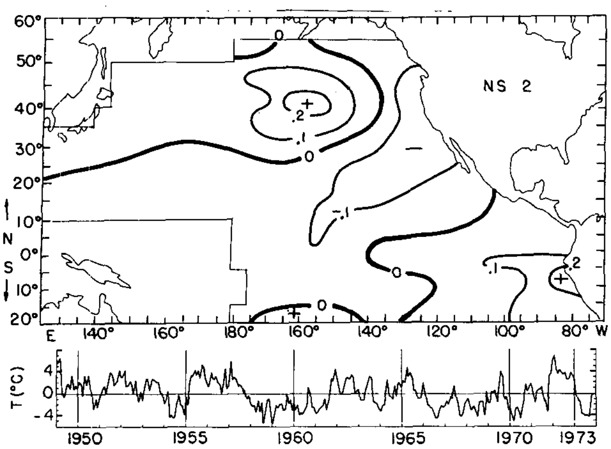

FIG. 8. NS2 explaining 7.5% of the total variance as in Fig. 7.

the equator. Two evident physical factors are that the sun is overhead north of the equator, leading to a minimum in radiative heating, and that southeast trade winds west of Peru are stronger (Wyrtki and Meyers, 1975) which produce stronger upwelling, and therefore cooling.

We have seen that the pattern of S2 contains evidence of both El Niño and the seasonal oscillation. Elimination of the latter from the time series leads to a time series similar to that of NS1, which best characterizes the El Niño mode. It is noteworthy that there is a simultaneous heating (or cooling) of the entire eastern edge of the Pacific, in both hemispheres, and the equatorial region. Coupled with the high degree of coherency over the remainder of the ocean this fact suggests that El Niño is a large-scale inter-hemispheric phenomenon. Inspection of the time series suggests a quasi-periodicity of 3–5 years.

The task of determining the cause of El Niño is not primarily one of putting forth a heating mechanism. More importantly, it is one of suggesting a mechanism which is consistent with the vast quantity of evidence of the oceanographic and meteorological changes coincident with El Niño.

For example, it would seem necessary that any proposed mechanism have variations in time which can be related to the time series of NS1. Wyrtki (1973) has recently suggested a hypothesis that can be explored in this regard. He has argued that the El Niño heating is primarily related to changes in the advection of warm water into the eastern tropical Pacific region by the Equatorial Countercurrent. This current is associated with a minimum in the zonal wind near the equator. Wyrtki has found a positive correlation between the transport of this current, as inferred from monthly mean island sea level heights, and the sea temperatures near Peru. We have calculated the correlation coefficient between this countercurrent index and the time coefficients of NS1 for the entire record 1949–73. It reaches a maximum of 0.68 (significant at the 99.9% level) when the countercurrent leads the temperature by one month but is only slightly less at zero lag.

In addition, the geographic distribution of anomalously warm and cold water suggested by the pattern of NS1 may place constraints on the atmosphere during El Niño. For instance, simple physical arguments would suggest that the warmer water in the equatorial region during El Niño as shown in Fig. 7 would result in lower pressure for the region. This seems to be verified in 1972 by the observation of lower pressures than normal at Lima, Peru (Wooster and Guillen, 1974) and significantly (99% level) increased rainfall from the 1965–74 mean at stations in the Galapagos Islands (1°S, 90°W). In addition, using similar arguments, one would expect during El Niño that the North Pacific anticyclone would exhibit pressures higher than average or lie northward of its mean position over the broad region in the North Pacific having lower temperatures. Subjective estimates were made of the latitude of the North Pacific high for the years 1970–73 from the surface pressure analyses published by the Southwest Fisheries Center (Laurs, 1970–74). During the period from September 1971 through September 1972 the highs were significantly (95% level) north of the positions of the 1961–74 monthly means. Much more research is necessary to establish the validity and importance of these and other possible inferences based upon this empirical orthogonal function analysis.

For many years El Niño has been recognized as being closely related to, or indeed a part of, another phenomenon, the Southern Oscillation. The latter involves an exchange of mass between a broad region near Indonesia and that of the southeast Pacific. There is good visual agreement between the time series of NS1 and those of the empirical orthogonal functions of tropical pressure, temperature and rainfall for the period 1951–60 which Kidson (1975b) argues are measures of the Southern Oscillation. Similar agreement is found between NS1 and surface pressure departures at Darwin, Australia,

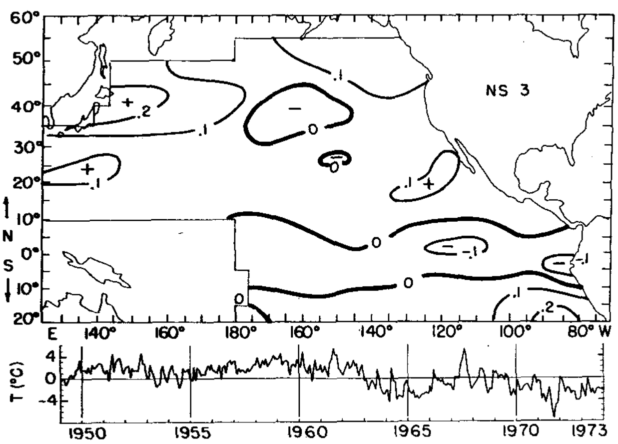

FIG. 9. NS3 explaining 5.8% of the total variance as in Fig. 7.

Unauthenticated | Downloaded 01/23/22 12:38 AM UTC

which Quinn and Burt (1970) used as a simple index of the Southern Oscillation.

An investigation of the causes of S3 is more tractable since this mode has sufficient annual periodicity so that it may be studied by using long-term monthly mean marine data which are probably far superior to those of individual year-months. We approach the problem by looking for a hypothesis which might explain the apparently anomalous warming in mid-winter in the region of 40°N, 170°W and the simultaneous cooling near 20°N, 140°E. We have calculated the meridional drift velocity in these two regions using the vorticity equation (Sverdrup, 1947) and the long-term seasonal average wind stress data compiled by Hellerman (1967) and assuming a mixed layer depth of 100 m. Table 2 indicates the estimates of this velocity in these regions for the four seasons. It is clear that in winter (DJF) the indicated southerly drift in the northern region and northerly drift in the southern region give the proper sign of the deviation. Such a drift at 40°N with the mean temperature gradients shown for February in Fig. 1 would give rise to an advective heating of about 0.013°C day^{-1} which is about half that required to model the changes in S3. The 6-month periodicity would appear to be the result of a simple coupling of this advection with the seasonal cycle illustrated in Fig. 3. These calculations do not, however, eliminate the possibility that other components of surface water heat balance, such as upwelling, are contributing significantly to S3.

We speculate that the S3 mode has a significant effect on the seasonal variations of Northern Hemisphere pressure and winds through a modulation of the semi-permanent Aleutian low. Kidson (1975a) has identified an empirical orthogonal function of Northern Hemisphere monthly mean sea level pressure which has a dominant 6-month periodicity, explaining approximately 3% of the total seasonal variance. This pressure function (denoted by Kidson as P3) has a center at

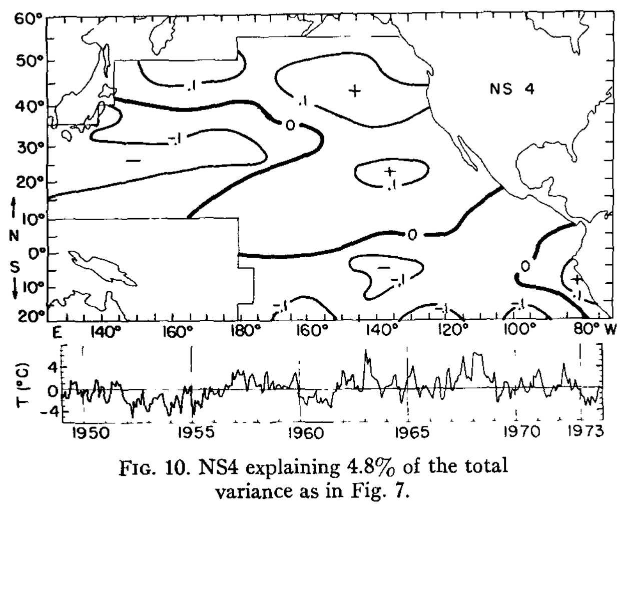

FIG. 10. NS4 explaining 4.8% of the total variance as in Fig. 7.

TABLE 2. Computed estimates of meridional ocean drift velocity (cm s^{-1}) for the four seasons for the 5° squares centered on the coordinates indicated (plus sign indicates southerly drift).

	Season			
	DJF	MAM	JJA	SON
42.5°N, 172.5°W	+2.1	−1.5	−2.1	−1.4
22.5°N, 142.5°E	−5.1	−2.0	−.4	+.6

60°N, 150°W and another center of opposite sign about 180° of longitude downstream. A comparison of the time series of S3 and P3 indicates that one month after the temperature of the S3 mode reaches a maximum in the North Pacific the pressure in the P3 mode reaches a minimum over the Pacific center. Similarly, one month after the temperature is a minimum the pressure is maximum. In addition, the geostrophic winds in the region of 40°N, 160°W, calculated from the 11-year monthly means of surface pressures (Clayton and Clayton, 1947) undergo a marked semi-annual variation with maxima in February and August. Although no conclusive statement may be made as to cause and effect, the relative positions of the centers of variation and the phase relationships suggest that the temperature changes induce the pressure and wind variations.

5. Conclusion

We have shown that empirical orthogonal analysis may be used to define modes of variation in the Pacific Ocean, north of 20°S. The most important of these modes have a large degree of spatial and temporal coherence suggesting that they may be closely related to the processes maintaining the heat balance of the ocean surface. At least three of these modes (S3, NS1, NS2) may also be associated with atmospheric variability on time scales of months to a few years. Finally, we believe such an analysis is an important step in creating as precise a mathematical description as possible of global oceanic and atmospheric parameters so that theoretical explanations of large-scale air-sea interactions may be more readily discerned.

Acknowledgments. We thank Minoru Tanaka for his calculation of the geostrophic winds and John Kidson for reviewing this manuscript. We also thank the Japan Meteorological Service, the Southwest Fisheries Center, the National Center for Atmospheric Research and Craig MacFarland, Director of the Charles Darwin Laboratory, for supplying data. This work was supported by the National Science Foundation, Atmospheric Sciences Section.

REFERENCES

Barnett, T. P., and R. E. Davis, 1975: Eigenvector analysis and prediction of sea surface temperature fluctuation in the northern Pacific Ocean. *Proc. WMO/IAMAP Symposium on Long-term Climatic Fluctuations*, Norwich, England, 439–450.

Unauthenticated | Downloaded 01/23/22 12:38 AM UTC

Clark, N. E., 1967: Report on an investigation of large-scale heat transfer processes and fluctuations of sea surface temperatures in the North Pacific Ocean. Ph.D. dissertation, M.I.T., 148 pp.

——, 1972: Specification of sea surface temperature anomaly patterns in the Eastern North Pacific. *J. Phys. Oceanogr.*, **2**, 391–404.

Clayton, H. H., and F. L. Clayton, 1947: *World Weather Records 1931–40.* Smithsonian Institution, Washington, D. C., 491–589.

Craddock, J. M., 1973: Problems and prospects for eigenvector analysis in meteorology. *The Statistician*, **22**, 133–45.

——, and C. R. Flood, 1969: Eigenvectors for representing the 500 mb geopotential surface over the Northern Hemisphere. *Quart. J. Roy. Meteor. Soc.*, **95**, 576–593.

Hellerman, S., 1967: An updated estimate of the wind stress on the world ocean. *Mon. Wea. Rev.*, **95**, 607–626; corrigendum, **96**, 62–74.

Iida, H., K. Katagiri, I. Maeda and E. Kamihira, 1975: On the normals of monthly sea surface temperatures from 1956 to 1970 for 5-degree squares in the western North Pacific Ocean. *Oceanogr. Mag.*, **26**, 73–89.

Kidson, J. W., 1975a: Eigenvector analysis of monthly mean surface data. *Mon. Wea. Rev.*, **103**, 177–186.

——, 1975b: Tropical eigenvector analysis and the Southern Oscillation. *Mon. Wea. Rev.*, **103**, 187–196.

Kutzbach, J. E., 1967: Empirical eigenvectors of sea level pressure, surface temperature and precipitation complexes over North America. *J. Appl. Meteor.*, **6**, 791–802.

Laurs, R. M., 1970–74: *Fishing Information.* Monthly, Southwest Fisheries Center, La Jolla, Calif.

Lorenz, E. N., 1956: Empirical orthogonal functions and statistical weather prediction. Sci. Rep. No. 1, Statist. Forecasting Project, Dept. Meteor., M.I.T., 49 pp.

Namias, J., 1972: Experiments in objectively predicting some atmospheric and oceanic variables for the winter of 1971–72. *J. Appl. Meteor.*, **11**, 1164–1174.

——, 1973: Collaboration of ocean and atmosphere in weather and climate. *Proc. 9th Annual Conf. Marine Tech. Soc.*, 163–178.

——, 1974: Longevity of a coupled air-sea-continent system. *Mon. Wea. Rev.*, **102**, 638–648.

Quinn, W. H., and W. V. Burt, 1970: Prediction of abnormally heavy precipitation over the equatorial Pacific dry zone. *J. Appl. Meteor.*, **9**, 20–28.

Rinne, J., 1971: Investigations of the forecasting error of a simple barotropic model with the aid of empirical orthogonal functions, Parts I and II. *Geophysica*, **11**, 185–240.

Rogers, J. C., 1974: Sea surface temperature anomalies in the eastern north Pacific and associated wintertime atmospheric fluctuations over North America—1960–73. *Bull. Amer. Meteor. Soc.*, **55**, 875.

Sette, O., J. Laurs and L. Eber, 1968: Monthly mean charts, sea-surface temperature North Pacific Ocean, 1949–62. *Bur. Commer. Fish. Circ.*, No. 258, pp. i–vi.

Sverdrup, H. V., 1947: Wind driven currents in a baroclinic ocean: with application to the equatorial currents of the eastern Pacific. *Proc. U. S. Nat. Acad. Sci.*, **33**, 318–26.

Trenberth, K. E., 1974: A quasi-biennial standing wave in the Southern Hemisphere and interrelations with sea surface temperature. *Quart. J. Roy. Meteor. Soc.*, **101**, 55–74.

U. S. Navy, 1969: *Marine Climatic Atlas of the World.* NAVAIR 50-1C-54, Naval Weather Service Command, Monterey, Calif., 21 pp.

Weare, B. C., A. R. Navato and R. E. Newell, 1975: Empirical orthogonal analysis of Pacific sea surface temperatures. *Proc. WMO/IAMAP Symposium on Long-term Climatic Fluctuations*, Norwich, England, 167–174.

Wooster, W. S., and O. Guillen, 1974: Characteristics of El Niño in 1972. *J. Marine Res.*, **32**, 387–404.

Wyrtki, K., 1973: Teleconnections in equatorial Pacific Ocean. *Science*, **180**, 66–68.

——, and G. Meyers, 1975: The trade wind field over the Pacific Ocean. Part I. The mean field and the annual variation. Rept. HIG-75-1, University of Hawaii, 26 pp.

Unauthenticated | Downloaded 01/23/22 12:38 AM UTC